OPEN

# Memantine protects blood–brain barrier integrity and attenuates neurological deficits through inhibiting nitric oxide synthase ser$^{1412}$ phosphorylation in intracerebral hemorrhage rats: involvement of peroxynitrite-related matrix metalloproteinase-9/NLRP3 inflammasome activation

Xiaowei Chen[a,*], Xu Xiang[b,*], Teng Xie[a], Zhijun Chen[a], Yu Mou[b], Zixu Gao[c], Xun Xie[c], Min Song[c], Hui Huang[d], Ziyun Gao[d] and Min Chen[d]

**Memantine has demonstrated beneficial effects on several types of brain insults via therapeutic mechanisms mainly related to its activity as a receptor antagonist of N-methyl-D-aspartate. However, the influences of memantine on intracerebral hemorrhage (ICH) remain obscure. This research probed into the neurovascular protective mechanisms of memantine after ICH and its impacts on neuronal nitric oxide synthase (nNOS) ser$^{1412}$ phosphorylation. ICH model was established by employing intrastriatal collagenase injection in rats. After modeling, rats were then allocated randomly into sham-operated (sham), vehicle-treated (ICH+V), and memantine-administrated (ICH+M) groups. Memantine (20 mg/kg/day) was intraperitoneally administered 30 min after ICH and thenceforth once daily. Rats were dedicated at 0.25, 6, 12, 24 h, 3 and 7 d post-ICH for measurement of corresponding indexes. Behavioral changes, brain edema, levels of nNOS ser$^{1412}$ phosphorylation, peroxynitrite, matrix metalloproteinase (MMP)-9, NLRP3, IL-1β and numbers of dying neurons, as well as the cellular localization of gelatinolytic activity, were detected among the groups. Memantine improved the neurologic deficits and mitigated brain water content, levels of MMP-9, NLRP3, IL-1β and dying neurons. Additionally, treatment with memantine also reduced nNOS ser$^{1412}$ phosphorylation and peroxynitrite formation compared with the ICH+V group at 24 h after ICH. In situ zymography simultaneously revealed that gelatinase activity was primarily colocalized with vessel walls and neurons. We concluded that memantine ameliorated blood–brain barrier disruption and neurologic dysfunction in an ICH rat model. The underlying mechanism might involve repression of nNOS ser$^{1412}$ phosphorylation, as well as peroxynitrite-related MMP-9 and NLRP3 inflammasome activation. *NeuroReport* 32: 228–237** **Copyright © 2021 The Author(s). Published by Wolters Kluwer Health, Inc.**

**NeuroReport** 2021, **32**:228–237

**Keyword:blood–brain barrier, intracerebral hemorrhage, memantine, neuronal nitric oxide synthase, peroxynitrite**

[a]Department of Neurosurgery, the First People's Hospital of Jingmen City, [b]Department of Neurosurgery, Jingmen Clinical Medical School, Hubei Minzu University, Hubei Province, [c]The Second Clinical Medical College of Nanchang University and [d]Department of Neurosurgery, The Second Affiliated Hospital of Nanchang University, Nanchang, Jiangxi Province, China

Correspondence to Dr. Min Chen, Department of Neurosurgery, The Second Affiliated Hospital of Nanchang University, 1 Minde Road, Donghu District, Nanchang 330008, China
Tel: +86 18296320726; e-mail: chen85min@126.com

*Xiaowei Chen and Xu Xiang contributed equally to the writing of this article.

**Received** 13 June 2020 **Accepted** 5 October 2020

## Introduction

Intracerebral hemorrhage (ICH) is the most menacing subtype of stroke and has an extremely poor prognosis. Nearly one-third of ICH patients die within 1 month following ICH and a large proportion of survivors remain disabled [1,2]. ICH is accompanied by the production of abundant free radicals (e.g., reactive oxygen species and reactive nitrogen species, namely ROS and RNS), which lead to blood–brain barrier (BBB) disruption, resulting in secondary edema in the brain and poor neurological deficits [3]. Besides, ICH-related free radicals also trigger inflammatory cascade involved with the progression of secondary brain edema [4]. Notedly, the structure of the BBB unit is composed of a basement membrane, endothelial cells, matrix, astrocytes and neurons, and disruption of BBB integrity is directly bound up with the aggravation of brain edema and neurologic defects [5]. However, which free radicals have the most destructive action on neurovascular units, and their specific molecular mechanism is still unclear.

Peroxynitrite ($ONOO^-$), which is formed by the reaction of nitric oxide and superoxide in a diffusion-limited way [6]. Excessive accumulation of $ONOO^-$ can cause

This is an open-access article distributed under the terms of the Creative Commons Attribution-Non Commercial-No Derivatives License 4.0 (CCBY-NC-ND), where it is permissible to download and share the work provided it is properly cited. The work cannot be changed in any way or used commercially without permission from the journal.

Supplemental Digital Content is available for this article. Direct URL citations appear in the printed text and are provided in the HTML and PDF versions of this article on the journal's website, www.neuroreport.com.

0959-4965 Copyright © 2021 The Author(s). Published by Wolters Kluwer Health, Inc. DOI: 10.1097/WNR.0000000000001577

Copyright © 2021 Wolters Kluwer Health, Inc. Unauthorized reproduction of this article is prohibited.

a serious effect on the BBB integrity in various central nervous system (CNS) disorders, including ICH, bringing about an adverse prognosis [3,7]. Peroxynitrite can compromise the integrity of the BBB by suppressing the energy metabolism of the cell, attenuating the activity of $Na^+/K^+$-ATPase, and activating matrix metalloproteinases (MMPs) [6–9]. Importantly, recent researches reported that $ONOO^-$ implicates activation of NLRP3 (NOD-like receptor family, pyrin domain containing 3) inflammasome, which mediates the inflammatory cascade and secondary brain insults post-ICH [4].

Preceding studies have investigated that the excessive release of glutamate associated with neuronal cell damage in several CNS pathologies [10,11], concurrently revealing that accompanied pathophysiological processes mediate more glutamate formation correlated to the stimulation of N-methyl-D-aspartate receptors (NMDARs) [12,13]. It has been experimentally validated that nitric oxide was involved in mediating NMDA neurotoxicity [14]. Furthermore, three neuronal nitric oxide synthase (NOS) isoforms including endothelial NOS, neuronal NOS, and inducible NOS are known to produce nitric oxide, and potent evidence hints that a particular causality exists between nNOS and NMDARs which closely related to glutamate excitotoxicity and subsequent neural damage [15,16].

Large amounts of glutamate is released during the pathophysiology of distinct CNS disorders, leading to NMDAR stimulation [17]. Memantine, the NMDAR antagonist, has recently demonstrated a powerful brain-protective effect in the treatment of disparate CNS diseases such as cerebral ischemia [18,19], infantile rat hydrocephalus [20], traumatic brain injury [21,22] and subarachnoid hemorrhage [16,23]. Overactivation of the complex of NMDAR, postsynaptic density protein 95 and nNOS produces large amounts of nitric oxide and superoxide anions ($O_2^-$), ultimately leading to the result of peroxynitrite formation [3,24]. More specifically, potent evidence indicated that nNOS phosphorylation at the site of Ser$^{1412}$ was responsible for the sustained peroxynitrite formation and the resultant neuronal loss [25].

Although above-mentioned evidences have depicted the protective function of memantine treatment in various CNS diseases, its impacts on nNOS and peroxynitrite as well as involved downstream targets after ICH remain unclear. The current study aimed to further clarify the treatment action of memantine on brain injury in ICH rats and determined probably involvement of the nNOS phosphorylation and peroxynitrite-related signaling pathway.

## Methods

### Animals

A total of 98 adult male Sprague-Dawley (SD) rats (6 rats died after surgery were eliminated) weighing between 250 and 300 g were purchased and utilized for our study. All the experimental procedures and protocols of the present study were authorized by the Ethics Committee of Nanchang University in conformity to the guidelines for the Care and Use of Laboratory Animals by the National Institutes of Health.

### Experimental groups, drugs and dose

Rats were randomly allocated to two separate experiments as described in Supplementary Figure 1, Supplement digital content 1, *http://links.lww.com/WNR/A611*. The experimental grouping information was blinded to the researchers and performers who conducted the behavioral scores and gelatinolytic activity tests as well as data analysis. Experiment 1 (Supplementary Figure 1, Supplement digital content 1, *http://links.lww.com/WNR/A611*) was set to study the time course of nNOS ser1412 and 3-nitrotyrosine (3-NT, a recognized hallmark of $ONOO^-$ production) in the ipsilateral brain tissues. Experiment 2 (Supplementary Figure 1, Supplement digital content 1, *http://links.lww.com/WNR/A611*) was established to probe into the effects of memantine on BBB integrity, brain edema and neurological deficits as well as related pathomechanism. Rats were randomly divided into three groups (1) sham group (surgery without ICH induction, $n$ = 18), (2) ICH+vehicle (ICH+V, $n$ = 18) group (saline treatment) and (3) ICH+ memantine group (ICH+M, $n$ = 18) group (memantine treatment). Rats in the ICH+M group received intraperitoneal memantine (Sigma-Aldrich, USA, St. Louis, Missouri, 20 mg/kg/day, prepared in freshly sterile saline) 30 min after the ICH induction in rats, then injected once daily until the rats were killed. The specific dose of memantine decided in our study was based on the previously published studies [26,27]. It is reported that 20 mg/kg memantine (intraperitoneal) can not only achieve effective brain concentration but also significantly attenuate brain inflammation and apoptosis, thus playing a neuroprotective role. An equivalent volume of saline instead of memantine was administrated in the ICH+V group.

### Intracerebral hemorrhage rat model

Male SD rats were anesthetized by intraperitoneal injection of pentobarbital sodium (45 mg/kg) and then fasten to a stereotaxic frame, just as mentioned before [4]. The heating pad was selected to maintain the animals' temperature at 36.5–37.3°C. A microsyringe needle inserted into the striatum after a burr hole was made by the stereotactic coordinates of 0.2 mm anterior, 2.8 mm lateral and 5.8 mm ventral to the bregma. ICH was induced by microinjection of 2 μL sterile saline containing 0.5 IU collagenase (Sigma-Aldrich) for more than 5 min. Then the burr hole was sealed, and the rats recovered under a comfortable environment with unstinted access to food and water.

### Behavioral testing

Behavioral testing was conducted by two investigators blinded to the groups at 24 and 72 h after ICH by using

Copyright © 2021 Wolters Kluwer Health, Inc. Unauthorized reproduction of this article is prohibited.

the modified neurological severity score (mNSS) [28]. The range of grades from 0 to 18 includes the tests of movement, sensation, reflexes and balance. The mNSS from 1 to 6 demonstrated mild injury, from 13 to 18 demonstrated severe injury and from 7 to 12 indicated the severity of injury in between.

### Blood–brain barrier integrity detection

BBB permeability was analyzed according to the foregoing research with small modifications [29]. The 5% Evan's blue solution was injected via tail vein to rats at 22 h after ICH. Cardiac perfusion was followed at 2 h after Evan's blue administration to eliminate the residual Evan's blue in the cerebral circulation. After the brain removed, a certain amount of N,N-dimethylformamide (DMF) was employed to isolate the hemispheres. The mixture liquid obtained followed by mechanically homogenized was kept in virtual darkness for 72 h at room temperature. The suspension was centrifuged for 30 min and Evan's blue content in the supernatant of tissue homogenates was spectrofluorimetrically analyzed. Leaky Evan's blue was demonstrated as micrograms per gram brain weight.

### Immunofluorescence

After anesthetized with pentobarbital sodium, the rats were perfused with PBS buffer solution and 4% paraformaldehyde transcardially, as described previously [30,31]. Once removed, the brains were successively postfixed, embedded and cut into slices. After deparaffinized, sections were microwaved in citrate buffer for antigen retrieval and incubated overnight at 4°C with the following primary antibodies: mouse monoclonal anti-3-NT antibody (Abcam, Cambridge, Massachusetts), rabbit polyclonal anti-MMP-9 antibody (Santa Cruz, California, USA), and rabbit polyclonal anti-CD68 (Abcam). After incubation with fluorescent conjugated secondary antibodies (Alexa Fluor 594 goat anti-mouse IgG, 1:500, Abcam; Alexa Fluor 488 goat anti-rabbit IgG, 1:500, Abcam) under room temperature for 1 h, the sections were restained by Hoechst 33258 for 10 min. The images were obtained by fluorescent microscopy (Bx51; Olympus Corporation, Shinjuku-ku, Japan).

### In situ zymography testing

The commercial kit was used to detect gelatinase MMP-9 in situ zymography as previously described (Shanghai, China) [30]. Fresh frozen sections with 10 μm thickness were incubated with gelatin conjugate at 4°C for 10 min and carried on for 1 h at 37°C. For double-staining, the tissue slices were incubated with primary antibodies for the labeling of neurons (NeuN, Abcam) and vessel basal lamina (fibronectin, Abcam) overnight at 4°C after the

**Fig. 1**

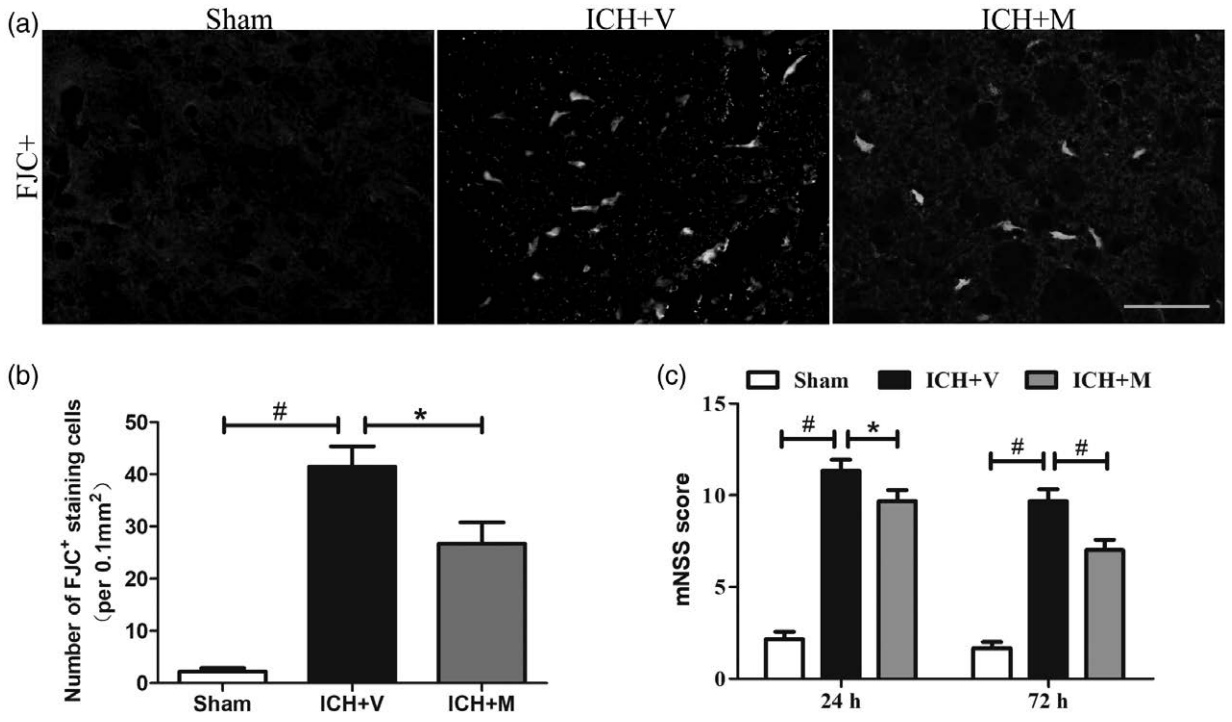


Effect of memantine on the number of FJC$^+$ neurons and neurological function scores. Degenerated neurons (a), quantitative analysis (b) and neurological scores (c). Fluoro–Jade staining demonstrated that administration of memantine markedly decreased neuron death compared with the vehicle group at 24 h post-ICH. Similarly, significantly lowered mNSS scores at 24 and 72 h of ICH rats with the treatment of memantine. $n = 6$ in each group. Data are presented as the mean ± SD. $^{\#}P < 0.05$, $^{*}P < 0.01$, scale bar = 50 μm. ICH, intracerebral hemorrhage; mNSS, modified neurological severity score.

Copyright © 2021 Wolters Kluwer Health, Inc. Unauthorized reproduction of this article is prohibited.

**Fig. 2**

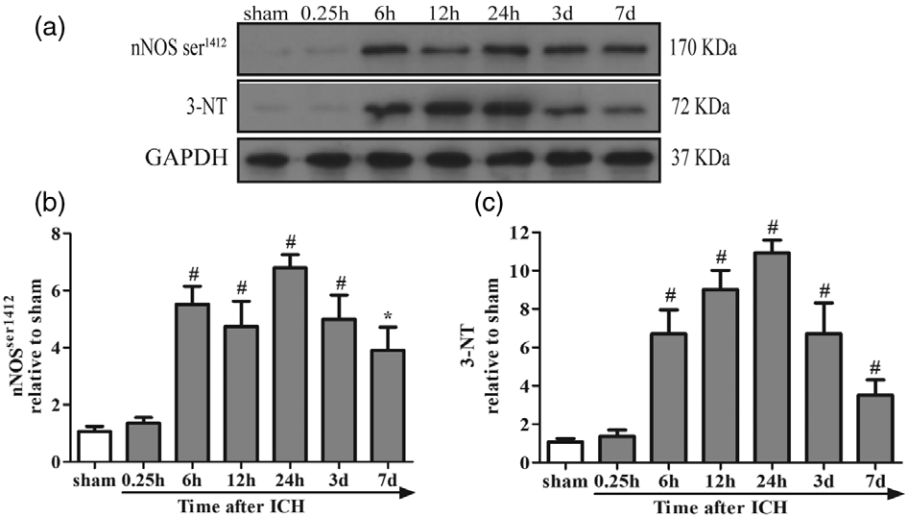


The expression of nNOS ser[1412] and 3-NT at different time points after ICH. (a) Western blot analysis and (b, c) densitometry. Western blot analysis of nNOS ser[1412] and $ONOO^-$ revealed that the expression trend of nNOS ser[1412] or 3-NT after ICH was basically consistent, and both of them reached the maximum at 24 h after ICH ($n = 4$). The molecular weight of nNOS ser[1412] and 3-NT was approximately 170 and 72 kDa, respectively. $^{\#}P < 0.05$, $^{*}P < 0.01$. ICH, intracerebral hemorrhage; nNOS, nitric oxide synthase; 3-NT, 3-nitrotyrosine.

gelatinolytic activity of various groups was quantified. Investigators were blinded to the experimental groups. The images were taken by the confocal microscope (OLYMPUS).

### Western blot analysis

The extraction of tissue protein in ipsilateral hemispheres tissues was performed following the instructions of the reagents kit and using RIPA buffer. The concentrations of protein were detected by the BCA Protein Assay Kit (Sigma-Aldrich). After divorced by the SDS-PAGE, the protein samples were transferred to a PVDF filter membrane. Following being blocked with 5% nonfat milk, primary antibodies (anti-phosphorylated nNOS at Ser[1214], Sigma-Aldrich; anti-3-nitrotyrosine, Abcam; anti-matrix metalloproteinase-9 (MMP-9), Abcam; ZO-1, Invitrogen, USA; NLRP3, Abcam; IL-1β, Abcam) were incubated respectively and followed by incubation with species-specific secondary antibodies (goat anti-mouse IgG 1:2000, Santa Cruz Biotechnology; goat anti-rabbit IgG 1:2000, Santa Cruz Biotechnology). Densitometry analysis was performed with Image J software after normalization to GAPDH.

### Statistical analysis

All data were shown as mean ± SD. Statistical analysis was performed using SPSS 20.0 software (SPSS, Chicago, Illinois, USA). Comparison among groups was determined via one-way analysis of variance and followed by the LSD or Dunnett's T3 test for the two groups' comparison within the multiple groups. Differences were considered to be statistically significant at $P < 0.05$.

## Result

### Treatment with memantine inhibits the neuronal death and ameliorates the behavioral function of rats after intracerebral hemorrhage

Fluoro–Jade staining method was applied to detect the dying neurons after ICH. As shown in Fig. 1a, b, the number of $FJC^+$ neurons was evidently increased at 24 h after ICH as compared with the sham group ($P < 0.05$). Administration of memantine notedly reduced neuronal death compared with the vehicle group ($P < 0.01$). Next, we adopted the mNSS tests to evaluate the neurological function (Fig. 1c). The mNSS scores were significantly increased at 24 and 72 h after ICH attack as compared with the sham group ($P < 0.01$). In contrast, memantine treatment evidently ameliorated the neurological deficits at the above time points ($P < 0.05$).

### Time course expression levels of neuronal nitric oxide synthase ser1412 and 3-nitrotyrosine after intracerebral hemorrhage

The expression levels of phosphorylated nNOS and 3-NT in the rat brain at designated time points (sham, 0.25, 6, 12, 24 h, 3 and 7 d post-ICH) were detected by western blot (Fig. 2a, b). nNOS ser[1412] level sharply increased as early as 6 h after ICH and showed a relative reduction at 12 h, peaked at 24 h and then diminished gradually. Despite falling evidently at 7 days, it was still higher than the sham group. Significant differences exist between ICH groups and sham groups at the above time points ($P < 0.05$). In contrast to nNOS ser1412, 3-NT level in the injured brain tissues also started to markedly increase as early as 6 h post-ICH, peaked at 24 h and then diminished

Copyright © 2021 Wolters Kluwer Health, Inc. Unauthorized reproduction of this article is prohibited.

**Fig. 3**

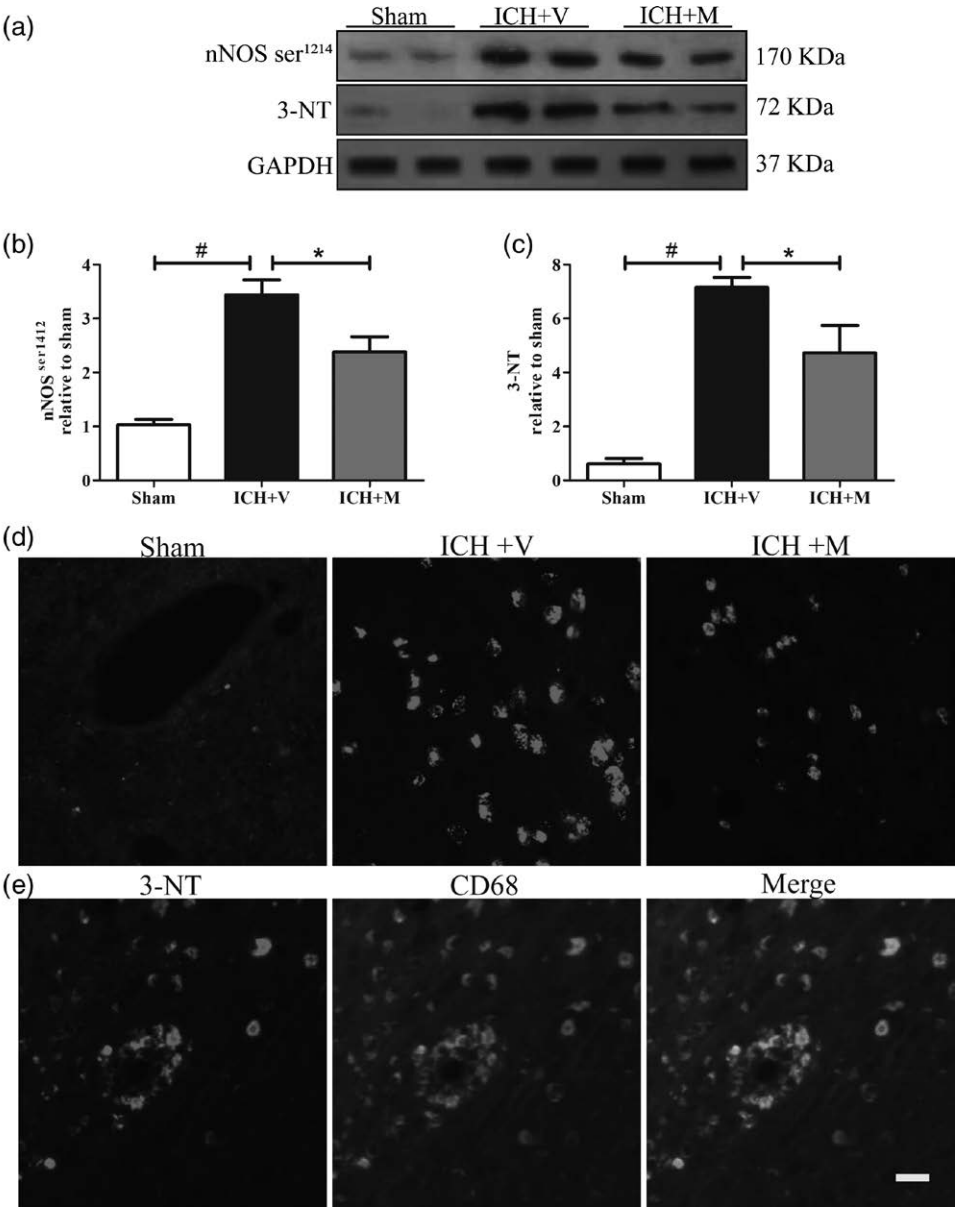


Treatment with memantine decreased the levels of nNOS Ser$^{1412}$ and 3-NT. (a)Western blot analysis. (b, c) Relative densities have been normalized against the sham group. (d) Immunofluorescence analysis. The vehicle group had an evident higher level of nNOS ser$^{1412}$ phosphorylation and 3-NT than the sham-operated group. Memantine treatment suppressed the elevation of nNOS ser$^{1412}$ phosphorylation and 3-NT when compared to the vehicle group at 24 h post-ICH. The molecular weight of nNOS ser$^{1412}$ and 3-NT was approximately 170 and 72 kDa, separately. (e) Double labeling of 3-NT and CD-68 showed that the formation of 3-NT is mainly localized in CD68 positive cells. $n = 6$ in each group. Data are presented as the mean ± SD. $^{\#}P < 0.05$, $^{*}P < 0.01$, scale bar = 50 μm. ICH, intracerebral hemorrhage; nNOS, nitric oxide synthase; 3-NT, 3-nitrotyrosine.

slowly. Similar to nNOS ser1412, it was still higher than the sham group at 7 days. The differences were statistically significant at the indicated time points ($P < 0.01$).

### Memantine decreased the phosphorylation of neuronal nitric oxide synthase at ser1412 and inhibited peroxynitrite formation following intracerebral hemorrhage

Phosphorylation of nNOS at ser$^{1412}$ is closely associated with nitric oxide production attributed to the increased nNOS activity, resulting in disruption of the BBB [32]. We determined if memantine inhibited nNOS ser$^{1412}$ phosphorylation, nNOS activity and subsequent pathway. By western blot (Fig. 3a, b, c), the levels of phosphorylated ser$^{1412}$ and peroxynitrite were remarkably elevated at 24 h after ICH. Whereas memantine administration effectively decreased the levels of NOS ser$^{1412}$ phosphorylation and peroxynitrite. By immunofluorescence, we also found that memantine treatment markedly reduced the expression of peroxynitrite

Copyright © 2021 Wolters Kluwer Health, Inc. Unauthorized reproduction of this article is prohibited.

**Fig. 4**

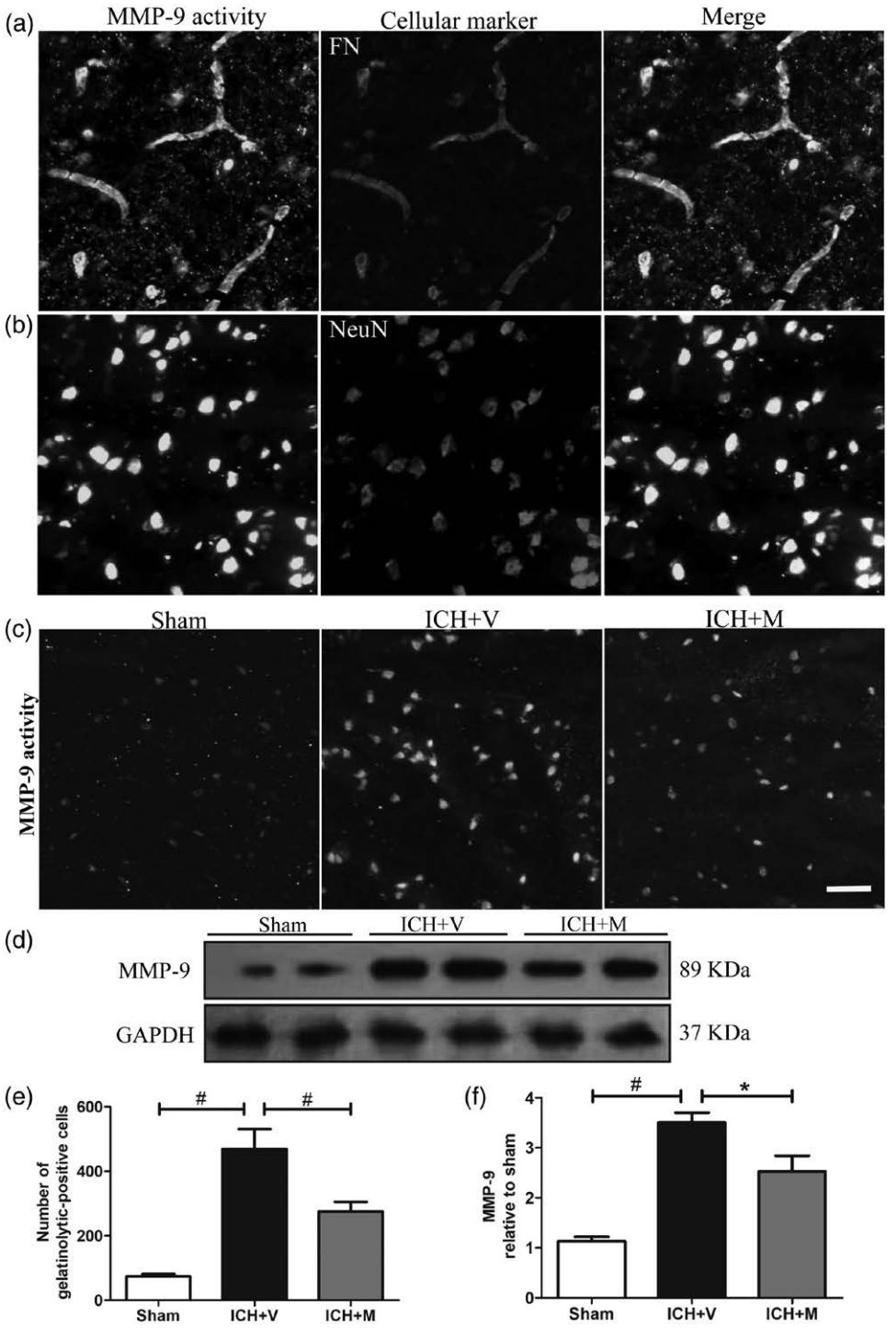


Cellular localization of MMP-9 activity and effect of memantine on MMP-9 activity and protein expression following ICH. The result of colocalization indicated that MMP-9 enzymatic activity was primarily detected in $FN^+$ vessel walls (a) and $NeuN^+$ neurons (b) following ICH. Original magnification, ×600. In situ zymography and quantitative analysis (c, e, $n = 6$), western blot and densitometric analysis (d, f, $n = 4$). Administration with memantine remarkably attenuated MMP-9 expression and gelatinolytic-positive cell numbers compared with the vehicle-treated group at 24 h after ICH ($P < 0.01$). The molecular weight of MMP-9 was approximately 89 kDa. Data are presented as the mean ± SD. $^{\#}P < 0.05$, $^{*}P < 0.01$, scale bar = 50 μm. ICH, intracerebral hemorrhage; MMP, matrix metalloproteinases.

Copyright © 2021 Wolters Kluwer Health, Inc. Unauthorized reproduction of this article is prohibited.

**Fig. 5**

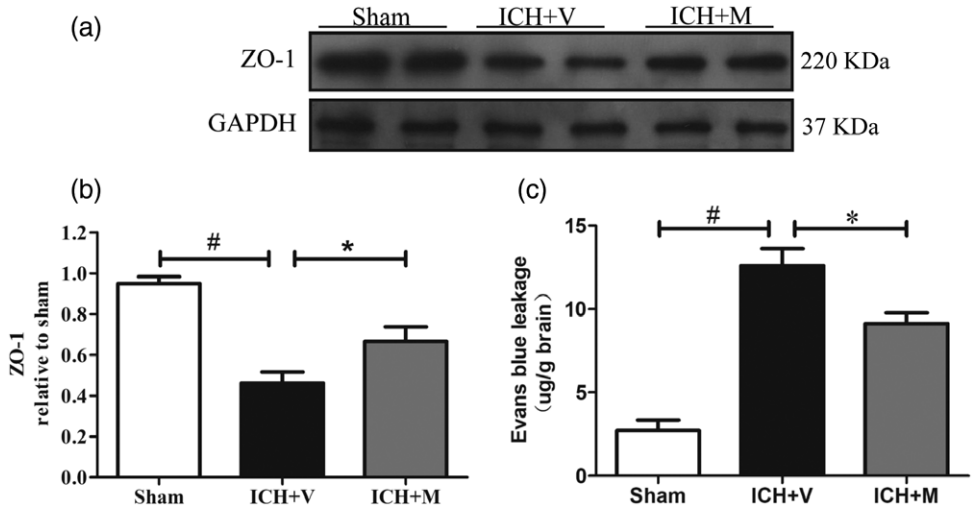


Influence of memantine on the expression of zonula occludens-1 (ZO-1) and BBB permeability. Western blot (a) and quantitation (b, $n = 4$) as well as Evan's blue measurement (c, $n = 6$). Memantine treatment significantly increased the expression of ZO-1 and attenuated the leakage of Evan's blue in the damaged brain tissues of rats compared with the vehicle group. Bands for ZO-1 migrated at approximately 220 kDa. Data are presented as mean ± SD. $^{\#}P < 0.05$, $^{*}P < 0.01$. BBB, blood–brain barrier.

**Fig. 6**

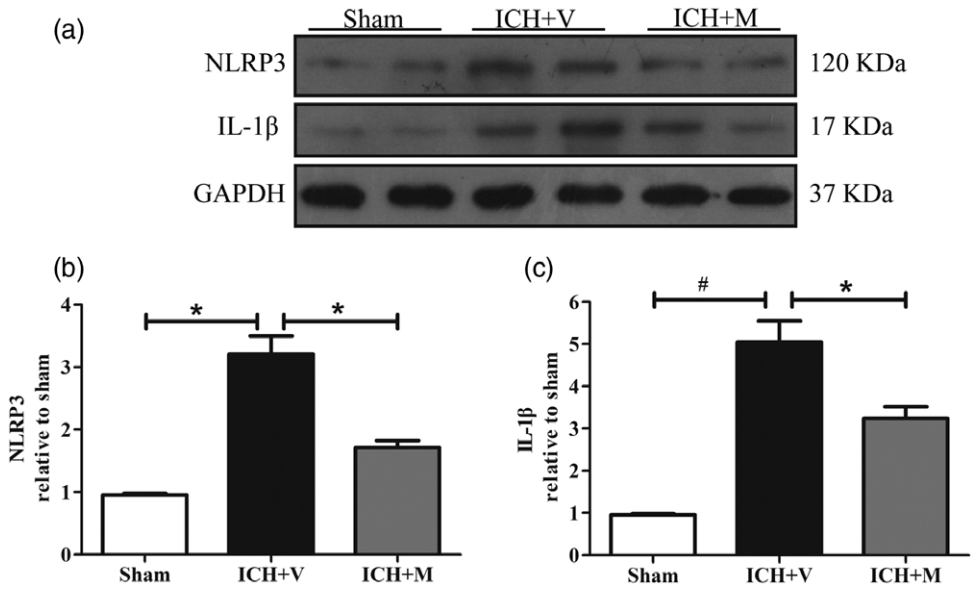


Effect of memantine injection on the protein levels of NLRP3 and IL-1β. Western blot (a) and densitometric analysis (b, c, $n = 4$). Injection with memantine remarkably suppressed the increases of NLRP3 and IL-1β compared with the vehicle-treated group at 24 h after ICH. The molecular weight of NLRP3 and IL-1β was approximately 120 and 17 kDa, separately. Data are presented as the mean ± SD. $^{\#}P < 0.05$, $^{*}P < 0.01$. ICH, intracerebral hemorrhage.

compared with the ICH+V group at 24 h post-ICH (Fig. 3d). Fluorescent double-labeling indicated that the formation of 3-NT was mainly localized in CD68 positive microglia/macrophages (Fig. 3e) ($P < 0.01$).

### Cellular localization of gelatinolytic activity following intracerebral hemorrhage

As shown by gelatin in situ zymography, colocalization of gelatinolytic activity and cell markers revealed that MMP-9 enzymatic activity was primarily observed in

Copyright © 2021 Wolters Kluwer Health, Inc. Unauthorized reproduction of this article is prohibited.

$FN^+$ vessel walls and $NeuN^+$ neurons (Fig. 4a, b). These tests showed that gelatinolytic activity could be activated in a wide range of cell types, including vessel walls and neurons, with consequently detrimental effects following ICH.

#### Treatment with memantine downregulated the increased MMP-9 activity and protein expression

MMP-9 played an important role in maintaining BBB integrity and we, therefore, investigated MMP-9 levels using in situ zymography(Fig. 4c, e) and western blot (Fig. 6d, f). The gelatinolytic activity and protein expression of MMP-9 was dramatically increased at 24 h after ICH. Whereas treatment with memantine markedly attenuated the MMP-9 protein levels and quantities of gelatinolytic-positive cells and vessels when compared with the vehicle-treated group ($P < 0.01$).

#### Administration with memantine attenuated the destruction of tight junction protein zonula occludens-1 and ameliorated the blood–brain barrier permeability

The integrity of the BBB requires the support of tight junction proteins [e.g., zonula occludens-1 (ZO-1)]. Thus, using western blot (Fig. 5a, b), we investigated whether memantine protects BBB via the modulation of ZO-1. The ZO-1 was evidently reduced at 24 h after ICH attack compared with the sham group. Contrarily, administration with memantine notably counteracted the ICH-mediated decreasing expression of ZO-1 compared to the ICH+V group ($P < 0.05$). Furtherly, we compared the exosmotic Evan's blue intensity between the memantine and the vehicle group. At 24 h post-ICH, memantine administration markedly attenuated BBB leakage and ameliorated the BBB permeability when compared with the vehicle group (Fig. 5c) ($P < 0.01$).

#### Treatment with memantine repressed the activation of NLRP3 and subsequent IL-1β production

The activation of NLRP3 inflammasome and the associated inflammatory cascade is bound up with the hemorrhagic brain injury. Current results demonstrated that at 24 h after ICH induction, the protein levels of NLRP3 and IL-1β were significantly enhanced, and memantine injection remarkably weakened the increases of NLRP3 and IL-1β (Fig. 6a, b, c, $P < 0.05$).

## Discussion

Following ICH, the hematoma degradation products trigger inflammatory responses in the perihematomal region [33]. Activation of glial cells, including astrocytes and microglia, is followed by the initiation of inflammatory responses and induction of proinflammatory and neurotoxic mediators, leading to BBB disruption and subsequent brain edema, neural apoptosis and impaired neurologic outcomes [34–36]. We, therefore, attempted to characterize the actions of memantine on the neurologic impairment, apoptosis of cells, nNOS and peroxynitrite formation, BBB integrity and related mechanisms in ICH rats.

As the reaction between nitric oxide and superoxide anions ($O_2^-$) and consequent oxidative product, peroxynitrite has been reported to feature in a wide variety of biological processes related to cell damage, destruction of BBB integrity, endothelial dysfunction and neurodegeneration, and is consequently correlated with a poor prognosis [37–39].

Although relevant researches have confirmed that the upregulation of iNOS increased the production of nitric oxide, iNOS was not detectable until 1 day after ICH [40]. Accompany with elevated glutamate concentration in the early phase of ICH, nNOS was aberrantly activated and exerted a dominant role in the formation of nitric oxide and $O_2^-$, thereby resulting in the sustained production of peroxynitrite [30]. Given that peroxynitrite formation is closely relevant to glutamate concentration and BBB disruption, our study revealed that memantine salvaged the BBB disruption by suppressing nNOS activation and peroxynitrite formation as well as underlying pathogenic targets.

The nNOS has been implicated in the breakdown of BBB integrity in several diseases, including heat stress-induced brain injury [41], transient cerebral ischemia [42] and subarachnoid hemorrhage [16]. Regarding the role of peroxynitrite, we previously revealed that $ONOO^-$ may mediate the activation of MMP-9 by two principal mechanisms. Specifically, it may upregulate nuclear factor-κB (NF-κB) expression indirectly and eventually modify MMP-9 transcription or may affect pro-MMP-9 directly, leading to significantly increased release of MMP-9 [43,44]. The activation of transcriptional and translational pathways regulates the expression of MMP-9 via relevant element-binding sites of functional enhancer, including NF-κB and activator protein-1 [45–47]. Increasing evidence have shown that MMPs exert a biological role in CNS diseases, including ICH [48,49], and peroxynitrite-mediated activation of MMP-9 has been predominantly linked to tight junction proteins degradation, BBB disruption and tissue damage [50,51]. In the setting of ischemic [25] and hemorrhagic storke [32] model, enhanced phosphorylation of nNOS at $Ser^{1412}$ was closely associated with the increased nNOS activity and subsequent nitric oxide production, which ultimately results in the excessive formation of $ONOO^-$. Inhibition of nNOS phosphorylation at $Ser^{1412}$ led to decreased levels of $ONOO^-$ [25]. In addition, it is reported that levels of phosphorylated $Ser^{1412}$ were elevated as early as 1 h after cerebral ischemia-reperfusion [34,52,53]. In this context, we discovered that the nNOS exerted detrimental effects through nNOS ser$^{1412}$ phosphorylation and nitric oxide overproduction as well as the resultant formation of $ONOO^-$, which collaborated with MMP-9 and negatively contributed to BBB disruption and neuronal damage after ICH.

Copyright © 2021 Wolters Kluwer Health, Inc. Unauthorized reproduction of this article is prohibited.

NLRP3 inflammasome, which was consisted of an NLRP3 scaffold, adaptor apoptosis speck-like protein (ASC) and the effector procaspase-1 [54], played a pivotal role in cerebrovascular diseases and have been reported to mediate BBB destruction and increased brain edema after cerebral ischemia [55,56]. More significantly, recent reports have shown that NLRP3 can be activated by reactive oxygen species (including peroxynitrite), Ca2+ signaling, and mitochondrial dysfunction [4]. Our results indicated that enhanced NLRP3 and IL-1β evidently decreased after memantine treatment, indicating that memantine can inhibit the inflammatory processes, which was in accord with the previous results [57,58]. Intriguingly, recent evidence demonstrated that the NLRP3-caspase-1 inflammasome directly activates MMP-9 by cleaving its N-terminal inhibitory domain. Genetic knockdown or inhibition of NLRP3 remarkably diminished the cleavage and activation of MMP-9 as well as mitigated the aortic destruction in a mice model of sporadic aortic aneurysm and dissection [59].

Memantine has been reported to exert an antagonistic effect on NMDARs, and to inhibit the $Ca^{2+}$-dependent cascade and nNOS signaling during the pathologic activation of NMDARs [60]. Previous studies showed that memantine had neuroprotective effects against several diseases, including Alzheimer's disease [61], hypoxia/ischemia [26], neuropathic pain [62] and Parkinsonism [26]. The relevant mechanisms are related to the attenuation of active caspase-3 levels and cell apoptosis, and the prevention of endothelial excitotoxicity, as well as the suppression of endogenous tPA upregulation. Notably, tissue plasminogen activator (tPA) is a selective activator of NMDA receptor-dependent signaling and neurotoxicity [63] and has been recognized as a promoter of MMP-9 activation and resultant hematoma expansion after ICH [57]. Surprisingly, memantine also exerted a powerful inhibitory action on the upregulation of tPA and ultimately reduced the MMP-9 level in the hemorrhagic brain [57]. The present research focused on the protective effect of memantine on BBB integrity within an ICH model, and revealed that it acted via a certain mechanism related to NMDAR antagonism, leading to the inhibition of nNOS $ser^{1412}$ phosphorylation, decreased nNOS signaling and subsequently decreased production of peroxynitrite, MMP-9 and NLRP3.

Collectively, although other factors may also be implicated in the decreases of nNOS activation and peroxynitrite formation, the current results suggested that the inhibitory effect of memantine on nNOS$ser^{1412}$ phosphorylation and peroxynitrite-related MMP-9 and NLRP3 activation may, at least, in part help to prevent BBB disruption and neurological deficits in ICH rats.

## Acknowledgements

This study was supported by the National Natural Science Foundation of China (Nos. 81760224), Youth Science Foundation of Jiangxi Province (20171BAB215019), Science and technology research Foundation of Jiangxi Provincial department of education (GJJ160123), and Foundation of Jiangxi health and Family Planning Commission (20185081). This study was also supported by Nature Science Foundation of Hubei Province (No.2019CFC863).

### Conflicts of interest

There are no conflicts of interest.

## References

1 You S, Zheng D, Delcourt C, Sato S, Cao Y, Zhang S, *et al*. Determinants of early versus delayed neurological deterioration in intracerebral hemorrhage. *Stroke* 2019; **50**:1409–1414.
2 Cordonnier C, Demchuk A, Ziai W, Anderson CS. Intracerebral haemorrhage: current approaches to acute management. *Lancet* 2018; **392**:1257–1268.
3 Ding R, Feng L, He L, Chen Y, Wen P, Fu Z, *et al*. Peroxynitrite decomposition catalyst prevents matrix metalloproteinase-9 activation and neurovascular injury after hemoglobin injection into the caudate nucleus of rats. *Neuroscience* 2015; **297**:182–193.
4 Zeng J, Chen Y, Ding R, Feng L, Fu Z, Yang S, *et al*. Isoliquiritigenin alleviates early brain injury after experimental intracerebral hemorrhage via suppressing ROS- and/or NF-κB-mediated NLRP3 inflammasome activation by promoting Nrf2 antioxidant pathway. *J Neuroinflammation* 2017; **14**:119.
5 Abbott NJ, Patabendige AA, Dolman DE, Yusof SR, Begley DJ. Structure and function of the blood-brain barrier. *Neurobiol Dis* 2010; **37**:13–25.
6 Qayyum I, Zubrow AB, Ashraf QM, Kubin J, Delivoria-Papadopoulos M, Mishra OP. Nitration as a mechanism of Na+, K+-ATPase modification during hypoxia in the cerebral cortex of the guinea pig fetus. *Neurochem Res* 2001; **26**:1163–1169.
7 Chen H, Chen X, Luo Y, Shen J. Potential molecular targets of peroxynitrite in mediating blood-brain barrier damage and haemorrhagic transformation in acute ischaemic stroke with delayed tissue plasminogen activator treatment. *Free Radic Res* 2018; **52**:1220–1239.
8 Suofu Y, Clark J, Broderick J, Wagner KR, Tomsick T, Sa Y, Lu A. Peroxynitrite decomposition catalyst prevents matrix metalloproteinase activation and neurovascular injury after prolonged cerebral ischemia in rats. *J Neurochem* 2010; **115**:1266–1276.
9 Cassina A, Radi R. Differential inhibitory action of nitric oxide and peroxynitrite on mitochondrial electron transport. *Arch Biochem Biophys* 1996; **328**:309–316.
10 Hillered L, Vespa PM, Hovda DA. Translational neurochemical research in acute human brain injury: the current status and potential future for cerebral microdialysis. *J Neurotrauma* 2005; **22**:3–41.
11 Arundine M, Tymianski M. Molecular mechanisms of calcium-dependent neurodegeneration in excitotoxicity. *Cell Calcium* 2003; **34**:325–337.
12 Choi DW. Glutamate neurotoxicity and diseases of the nervous system. *Neuron* 1988; **1**:623–634.
13 Sarrafzadeh A, Haux D, Küchler I, Lanksch WR, Unterberg AW. Poor-grade aneurysmal subarachnoid hemorrhage: relationship of cerebral metabolism to outcome. *J Neurosurg* 2004; **100**:400–406.
14 Iadecola C. Bright and dark sides of nitric oxide in ischemic brain injury. *Trends Neurosci* 1997; **20**:132–139.
15 Sehba FA, Chereshnev I, Maayani S, Friedrich V Jr, Bederson JB. Nitric oxide synthase in acute alteration of nitric oxide levels after subarachnoid hemorrhage. *Neurosurgery* 2004; **55**:671–677.
16 Huang CY, Wang LC, Wang HK, Pan CH, Cheng YY, Shan YS, *et al*. Memantine alleviates brain injury and neurobehavioral deficits after experimental subarachnoid hemorrhage. *Mol Neurobiol* 2015; **51**:1038–1052.
17 Tanaka A, Ito Y, Kawasaki H, Kitabayashi C, Nishioka R, Yamazato M, *et al*. Effects of memantine on nitric oxide production and hydroxyl radical metabolism during cerebral ischemia and reperfusion in mice. *J Stroke Cerebrovasc Dis* 2018; **27**:1609–1615.
18 Liu Y, Huang Y, Xu Y, Qu P, Wang M. Memantine protects against ischemia/reperfusion-induced brain endothelial permeability. *IUBMB Life* 2018; **70**:336–343.
19 Gu SX, Sonkar VK, Katare PB, Kumar R, Kruger WD, Arning E, *et al*. Memantine protects from exacerbation of ischemic stroke and blood brain barrier disruption in mild but not severe hyperhomocysteinemia. *J Am Heart Assoc* 2020; **9**:e013368.

Copyright © 2021 Wolters Kluwer Health, Inc. Unauthorized reproduction of this article is prohibited.

20 Cabuk B, Etus V, Bozkurt SU, Sav A, Ceylan S. Neuroprotective effect of memantine on hippocampal neurons in infantile rat hydrocephalus. *Turk Neurosurg* 2011; **21**:352–358.
21 Abrahamson EE, Poloyac SM, Dixon CE, Dekosky ST, Ikonomovic MD. Acute and chronic effects of single dose memantine after controlled cortical impact injury in adult rats. *Restor Neurol Neurosci* 2019; **37**:245–263.
22 Mei Z, Qiu J, Alcon S, Hashim J, Rotenberg A, Sun Y, *et al*. Memantine improves outcomes after repetitive traumatic brain injury. *Behav Brain Res* 2018; **340**:195–204.
23 Luo F, Wu L, Zhang Z, Zhu Z, Liu Z, Guo B, *et al*. The dual-functional memantine nitrate MN-08 alleviates cerebral vasospasm and brain injury in experimental subarachnoid haemorrhage models. *Br J Pharmacol* 2019; **176**:3318–3335.
24 Lai TW, Zhang S, Wang YT. Excitotoxicity and stroke: identifying novel targets for neuroprotection. *Prog Neurobiol* 2014; **115**:157–188.
25 Khan M, Dhammu TS, Matsuda F, Singh AK, Singh I. Blocking a vicious cycle nNOS/peroxynitrite/AMPK by S-nitrosoglutathione: implication for stroke therapy. *BMC Neurosci* 2015; **16**:42.
26 Chen HS, Wang YF, Rayudu PV, Edgecomb P, Neill JC, Segal MM, *et al*. Neuroprotective concentrations of the N-methyl-D-aspartate open-channel blocker memantine are effective without cytoplasmic vacuolation following post-ischemic administration and do not block maze learning or long-term potentiation. *Neuroscience* 1998; **86**:1121–1132.
27 Sinn DI, Lee ST, Chu K, Jung KH, Song EC, Kim JM, *et al*. Combined neuroprotective effects of celecoxib and memantine in experimental intracerebral hemorrhage. *Neurosci Lett* 2007; **411**:238–242.
28 Shen LH, Li Y, Chen J, Cui Y, Zhang C, Kapke A, *et al*. One-year follow-up after bone marrow stromal cell treatment in middle-aged female rats with stroke. *Stroke* 2007; **38**:2150–2156.
29 Khan M, Sakakima H, Dhammu TS, Shunmugavel A, Im YB, Gilg AG, *et al*. S-nitrosoglutathione reduces oxidative injury and promotes mechanisms of neurorepair following traumatic brain injury in rats. *J Neuroinflammation* 2011; **8**:78.
30 Ding R, Chen Y, Yang S, Deng X, Fu Z, Feng L, *et al*. Blood-brain barrier disruption induced by hemoglobin in vivo: involvement of up-regulation of nitric oxide synthase and peroxynitrite formation. *Brain Res* 2014; **1571**:25–38.
31 Yang S, Chen Y, Deng X, Jiang W, Li B, Fu Z, *et al*. Hemoglobin-induced nitric oxide synthase overexpression and nitric oxide production contribute to blood-brain barrier disruption in the rat. *J Mol Neurosci* 2013; **51**:352–363.
32 Wada K, Osuka K, Watanabe Y, Usuda N, Fukasawa M, Araki Y, *et al*. Subarachnoid hemorrhage induces neuronal nitric oxide synthase phosphorylation at Ser1412 in the dentate gyrus of the rat brain. *Nitric Oxide* 2018; **81**:67–74.
33 Alm P, Sharma HS, Sjöquist PO, Westman J. A new antioxidant compound H-290/51 attenuates nitric oxide synthase and heme oxygenase expression following hyperthermic brain injury. An experimental study using immunohistochemistry in the rat. *Amino Acids* 2000; **19**:383–394.
34 Hara H, Huang PL, Panahian N, Fishman MC, Moskowitz MA. Reduced brain edema and infarction volume in mice lacking the neuronal isoform of nitric oxide synthase after transient MCA occlusion. *J Cereb Blood Flow Metab* 1996; **16**:605–611.
35 Sharma HS, Badgaiyan RD, Alm P, Mohanty S, Wiklund L. Neuroprotective effects of nitric oxide synthase inhibitors in spinal cord injury-induced pathophysiology and motor functions: an experimental study in the rat. *Ann N Y Acad Sci* 2005; **1053**:422–434.
36 Genovese T, Mazzon E, Esposito E, Muià C, Di Paola R, Bramanti P, Cuzzocrea S. Beneficial effects of FeTSPP, a peroxynitrite decomposition catalyst, in a mouse model of spinal cord injury. *Free Radic Biol Med* 2007; **43**:763–780.
37 Gu Z, Kaul M, Yan B, Kridel SJ, Cui J, Strongin A, *et al*. S-nitrosylation of matrix metalloproteinases: signaling pathway to neuronal cell death. *Science* 2002; **297**:1186–1190.
38 Rosenberg GA. Matrix metalloproteinases in neuroinflammation. *Glia* 2002; **39**:279–291.
39 Sato H, Kita M, Seiki M. v-Src activates the expression of 92-kDa type IV collagenase gene through the AP-1 site and the GT box homologous to retinoblastoma control elements. A mechanism regulating gene expression independent of that by inflammatory cytokines. *J Biol Chem* 1993; **268**:23460–23468.
40 Chiueh CC, Rauhala P. The redox pathway of S-nitrosoglutathione, glutathione and nitric oxide in cell to neuron communications. *Free Radic Res* 1999; **31**:641–650.
41 Muresanu DF, Sharma A, Patnaik R, Menon PK, Mössler H, Sharma HS. Exacerbation of blood-brain barrier breakdown, edema formation, nitric oxide synthase upregulation and brain pathology after heat stroke in diabetic and hypertensive rats. Potential neuroprotection with cerebrolysin treatment. *Int Rev Neurobiol* 2019; **146**:83–102.
42 Jiang Z, Li C, Arrick DM, Yang S, Baluna AE, Sun H. Role of nitric oxide synthases in early blood-brain barrier disruption following transient focal cerebral ischemia. *PLoS One* 2014; **9**:e93134.
43 Pacher P, Beckman JS, Liaudet L. Nitric oxide and peroxynitrite in health and disease. *Physiol Rev* 2007; **87**:315–424.
44 Wang J, Tsirka SE. Contribution of extracellular proteolysis and microglia to intracerebral hemorrhage. *Neurocrit Care* 2005; **3**:77–85.
45 Parathath SR, Parathath S, Tsirka SE. Nitric oxide mediates neurodegeneration and breakdown of the blood-brain barrier in tPA-dependent excitotoxic injury in mice. *J Cell Sci* 2006; **119**:339–349.
46 Phares TW, Fabis MJ, Brimer CM, Kean RB, Hooper DC. A peroxynitrite-dependent pathway is responsible for blood-brain barrier permeability changes during a central nervous system inflammatory response: TNF-alpha is neither necessary nor sufficient. *J Immunol* 2007; **178**:7334–7343.
47 Zhao X, Zhang Y, Strong R, Zhang J, Grotta JC, Aronowski J. Distinct patterns of intracerebral hemorrhage-induced alterations in NF-kappaB subunit, iNOS, and COX-2 expression. *J Neurochem* 2007; **101**:652–663.
48 Yong VW, Power C, Forsyth P, Edwards DR. Metalloproteinases in biology and pathology of the nervous system. *Nat Rev Neurosci* 2001; **2**:502–511.
49 Wang T, Chen X, Wang Z, Zhang M, Meng H, Gao Y, *et al*. Poloxamer-188 can attenuate blood-brain barrier damage to exert neuroprotective effect in mice intracerebral hemorrhage model. *J Mol Neurosci* 2015; **55**:240–250.
50 Wang J, Tsirka SE. Neuroprotection by inhibition of matrix metalloproteinases in a mouse model of intracerebral haemorrhage. *Brain* 2005; **128**:1622–1633.
51 Chen H, Guan B, Chen X, Chen X, Li C, Qiu J, *et al*. Baicalin attenuates blood-brain barrier disruption and hemorrhagic transformation and improves neurological outcome in ischemic stroke rats with delayed t-PA treatment: involvement of ONOO−MMP-9 pathway. *Transl Stroke Res* 2018; **9**:515–529.
52 Huang Z, Huang PL, Panahian N, Dalkara T, Fishman MC, Moskowitz MA. Effects of cerebral ischemia in mice deficient in neuronal nitric oxide synthase. *Science* 1994; **265**:1883–1885.
53 Gürsoy-Ozdemir Y, Can A, Dalkara T. Reperfusion-induced oxidative/nitrative injury to neurovascular unit after focal cerebral ischemia. *Stroke* 2004; **35**:1449–1453.
54 Wang Z, Zhang S, Xiao Y, Zhang W, Wu S, Qin T, *et al*. NLRP3 inflammasome and inflammatory diseases. *Oxid Med Cell Longev* 2020; **2020**:4063562.
55 Wang H, Chen H, Jin J, Liu Q, Zhong D, Li G. Inhibition of the NLRP3 inflammasome reduces brain edema and regulates the distribution of aquaporin-4 after cerebral ischaemia-reperfusion. *Life Sci* 2020; **251**:117638.
56 Xu F, Shen G, Su Z, He Z, Yuan L. Glibenclamide ameliorates the disrupted blood-brain barrier in experimental intracerebral hemorrhage by inhibiting the activation of NLRP3 inflammasome. *Brain Behav* 2019; **9**:e01254.
57 Lee ST, Chu K, Jung KH, Kim J, Kim EH, Kim SJ, *et al*. Memantine reduces hematoma expansion in experimental intracerebral hemorrhage, resulting in functional improvement. *J Cereb Blood Flow Metab* 2006; **26**:536–544.
58 Huang XT, Li C, Peng XP, Guo J, Yue SJ, Liu W, *et al*. An excessive increase in glutamate contributes to glucose-toxicity in β-cells via activation of pancreatic NMDA receptors in rodent diabetes. *Sci Rep* 2017; **7**:44120.
59 Ren P, Wu D, Appel R, Zhang L, Zhang C, Luo W, *et al*. Targeting the NLRP3 inflammasome with inhibitor MCC950 prevents aortic aneurysms and dissections in mice. *J Am Heart Assoc* 2020; **9**:e014044.
60 Chen B, Wang G, Li W, Liu W, Lin R, Tao J, *et al*. Memantine attenuates cell apoptosis by suppressing the calpain-caspase-3 pathway in an experimental model of ischemic stroke. *Exp Cell Res* 2017; **351**:163–172.
61 Parsons CG, Danysz W, Quack G. Memantine is a clinically well tolerated N-methyl-D-aspartate (NMDA) receptor antagonist–a review of preclinical data. *Neuropharmacology* 1999; **38**:735–767.
62 Lipton SA. Failures and successes of NMDA receptor antagonists: molecular basis for the use of open-channel blockers like memantine in the treatment of acute and chronic neurologic insults. *NeuroRx* 2004; **1**:101–110.
63 Parcq J, Bertrand T, Montagne A, Baron AF, Macrez R, Billard JM, *et al*. Unveiling an exceptional zymogen: the single-chain form of tPA is a selective activator of NMDA receptor-dependent signaling and neurotoxicity. *Cell Death Differ* 2012; **19**:1983–1991.


Copyright © 2021 Wolters Kluwer Health, Inc. Unauthorized reproduction of this article is prohibited.